

Natural mass hierarchy among three heavy Majorana neutrinos for resonant leptogenesis under modular A_4 symmetry

Dong Woo Kang,^{1,*} Jongkuk Kim,^{1,†} Takaaki Nomura,^{2,‡} and Hiroshi Okada^{3,4,§}

¹*School of Physics, KIAS, Seoul 02455, Korea*

²*College of Physics, Sichuan University, Chengdu 610065, China*

³*Asia Pacific Center for Theoretical Physics (APCTP) - Headquarters San 31,
Hyoja-dong, Nam-gu, Pohang 790-784, Korea*

⁴*Department of Physics, Pohang University of Science
and Technology, Pohang 37673, Republic of Korea*

(Dated: May 18, 2022)

Abstract

It is clear that matter is dominant in the Universe compared to antimatter. We call this problem baryon asymmetry. The baryon asymmetry is experimentally determined by both cosmic microwave background and big bang nucleosynthesis measurements. To resolve the baryon number asymmetry of the Universe as well as neutrino oscillations, we study a radiative seesaw model in a modular A_4 symmetry. Degenerate heavy Majorana neutrino masses can be naturally realized in an appropriate assignments under modular A_4 with large imaginary part of modulus τ , and it can induce measured baryon number via resonant leptogenesis that is valid in around TeV scale energy theory. We also find that the dominant contribution to the CP asymmetry arises from $\text{Re}[\tau]$ through our numerical analysis satisfying the neutrino oscillation data.

*Electronic address: dongwookang@kias.re.kr

†Electronic address: jkkim@kias.re.kr

‡Electronic address: nomura@scu.edu.cn

§Electronic address: hiroshi.okada@apctp.org

I. INTRODUCTION

Understanding the origin of the observed imbalance in baryonic matter remains one of the important problems, so-called Baryon Asymmetry of the Universe (BAU) problem, in particle physics and cosmology. The baryon abundance at present Universe obtained from Cosmic Microwave Background anisotropy and Big Bang Nucleosynthesis is [1]

$$\Omega_B h^2 = 0.0223 \pm 0.0002. \quad (\text{I.1})$$

This is related to the baryon asymmetry which is given by

$$Y_B \equiv \frac{n_B}{s} \simeq 0.86 \times 10^{-10}, \quad (\text{I.2})$$

where n_B is the number density of the baryon and s is entropy density.

Theoretically resolving the BAU is one of the important motivations to consider physics beyond the Standard Model (SM).¹ One attractive scenario is leptogenesis [4] that is intimately related to smallness of neutrino masses through canonical seesaw mechanism [5, 6] by introducing heavy Majorana fermions. The decay of the heavy Majorana neutrino creates lepton asymmetry and it is converted into baryon asymmetry by sphalerons around electroweak scale. In order to generate observed baryon asymmetry in Eq. (I.2), we need rather large mass of the Majorana neutrinos that is 10^{10} GeV at least. It implies that such heavy fermions could not be produced by any current collider experiments.

On the contrary, resonant leptogenesis [7, 8] is one of the promising candidates to explain BAU at low energy scale that could be around TeV scale being within the reach of current or near future experiments. In order to realize the resonant leptogenesis, we need two almost degenerate Majorana fermions at least.² Then, we have an enhancement of the CP asymmetry parameter [9] that can generate enough BAU even at low energy scale. The next task would be how to realize the almost degenerate masses, even though most of the endeavors set such a situation by hand unless symmetries are introduced.

¹ Even though there exists electroweak baryogenesis [2] within the context of SM, it would be almost ruled out due to requirement of too strong first order electroweak phase transition. Non-thermal WIMP baryogenesis is one of the fascinating mechanisms since re-annihilation of dark matter provides the observed baryon asymmetry as well as the correct relic density [3].

² More concretely, the maximum enhancement may be achieved if the mass splitting between two Majorana fermions is comparable to the decay width of either Majorana fermions.

Recently, a modular flavor symmetry was proposed in Ref. [10, 11]. The symmetry has additional quantum number that is called modular weight, and flavor structures of dimensionless couplings such as Yukawas are uniquely determined once the modular weights are fixed. As a result, more predictive models are possible compared to traditional flavor models. In fact, a plethora of scenarios have been studied after this idea up to now, especially applying modular A_4 symmetry [10, 12–63].³ More interestingly on the resonant leptogenesis, *two degenerate Majorana fermion masses are arisen at two fixed points of modulus $\tau = i, i\infty$, once we assign three Majorana fermions N^c to be triplet under A_4 with -1 modular weight!* These fixed points are statistically favored in the flux compactification of Type IIB string theory [52].⁴ Under the assignment, the Majorana mass matrix (M_N) is given by

$$M_N = M_0 \begin{bmatrix} 2y_1 & -y_3 & -y_2 \\ -y_3 & 2y_2 & -y_1 \\ -y_2 & -y_1 & 2y_3 \end{bmatrix}, \quad (\text{I.3})$$

where $Y_3^{(2)} \equiv (y_1, y_2, y_3)$ is A_4 triplet modular form with two modular weights appearing in Majorana mass term $\frac{1}{2}M_0 Y_3^{(2)} \overline{N^c} N$; concrete forms of modular forms are found in Appendix. In the limit of $\tau = i$, we have $(0, M_0, M_0)$ mass eigenvalues after the diagonalization of Eq. (I.3). The deviation from the $\tau = i$ gives small mass splitting of the two massive Majorana fermions as well as the small mass eigenvalue for the massless Majorana fermion. We naturally get the small mass splitting between two massive Majorana fermions but it is hard to realize resonant leptogenesis with one light (almost massless) Majorana fermion. In the limit of $\tau = i\infty$, on the other hand, we have $(M_0, M_0, 2M_0)$ mass eigenvalues, i.e. three heavy Majorana fermions with two degenerated one. And the deviation along the $\text{Im}[\tau]$ direction from the $\tau = i\infty$ provides small mass splitting of the lightest two massive Majorana fermions, while the deviation along the $\text{Re}[\tau]$ direction provides the CP asymmetry.

In this paper, we apply the modular A_4 symmetry with rather large $\text{Im}[\tau]$ to a supersymmetric radiative seesaw model, and discuss how to realize the neutrino oscillation data and BAU simultaneously [73]. Radiative seesaw model [74] is known as a promising candidate

³ Here, we provide useful review references for beginners [64–72].

⁴ Generally, there are three fixed points adding $\tau = e^{2\pi i/3}$. But this point does not give degenerated masses under the same assignment.

to explain the neutrino oscillation data at low energy scale, and connect the neutrinos and dark matter or new particles. Moreover, several interesting flavor physics such as lepton flavor violations (LFVs) potentially come into our discussion. Due to almost two degenerate Majorana fermions, the resonant leptogenesis is naturally realized and proper field assignments for modular weight assure the radiative seesaw model instead of an ad-hoc symmetry such as Z_2 that is introduced by hand.

Our manuscript is organized as follows. In Sec. II, we give our concrete model set up under A_4 modular symmetry, and formulate mass matrices of Majorana heavy neutrinos, inert scalar bosons, and active neutrinos. Then, we explain how to compare the experimental values. In Sec. III, we show how to realize the resonant leptogenesis in our model. In Sect. IV, we perform the χ^2 numerical analysis, and show our results to satisfy all the experimental constraints. Finally, we conclude and discuss in Sec. V.

II. MODEL

In this section, we review a radiative seesaw model in a modular A_4 symmetry. We introduce modular A_4 symmetry and assign $\{1, 1', 1''\}$ for $(\hat{L}_e, \hat{L}_\mu, \hat{L}_\tau)$ and $\{1, 1'', 1'\}$ for $(\hat{e}^c, \hat{\mu}^c, \hat{\tau}^c)$ in order to consider the mass eigenbasis of charged-lepton sector. Their modular weights are assigned to be $\{-2, -2, 0\}$ for each family. Note here that notation \hat{f} for a field f indicates matter chiral superfield including boson and fermion, otherwise f denotes boson or fermion with even R -parity. In addition, we introduce three electrically neutral superfields \hat{N}^c as discussed in introduction. Then, we add $\hat{\eta}_1$ with -3 modular weight whose corresponding scalar field is important to connect the active neutrinos and the Majorana fermions, while $\hat{\eta}_2$ is introduced only to cancel the gauge chiral anomaly and this field does not contribute to the neutrino sector.⁵ The field contents and their assignments are summarized in Table I.

⁵ \hat{H}_2 is requested by obtaining the SM Higgs mass through μ term. But, we suppose H_2 does not contribute to our main discussion as well.

	Matter super fields							
Fields	$(\hat{L}_e, \hat{L}_\mu, \hat{L}_\tau)$	$(\hat{e}^c, \hat{\mu}^c, \hat{\tau}^c)$	\hat{N}^c	\hat{H}_1	\hat{H}_2	$\hat{\eta}_1$	$\hat{\eta}_2$	$\hat{\chi}$
$SU(2)_L$	2	1	1	2	2	2	2	1
$U(1)_Y$	$\frac{1}{2}$	-1	0	$\frac{1}{2}$	$-\frac{1}{2}$	$\frac{1}{2}$	$-\frac{1}{2}$	0
A_4	$\{1, 1', 1''\}$	$\{1, 1'', 1'\}$	3	1	1	1	1	1
$-k$	$\{-2, -2, 0\}$	$\{-2, -2, 0\}$	-1	0	0	-3	-3	-3

TABLE I: Matter chiral superfields and their charge assignments under $SU(2)_L \times U(1)_Y \times A_4$, where $-k$ is the number of modular weight.

A. Majorana mass matrix

At first, we develop our discussion on the mass matrix of Majorana fermion N given in Eq. (I.3). At nearby $\tau = i\infty$, (y_1, y_2, y_3) is expanded by p_ϵ and given by $(1 + 12p_\epsilon, -6p_\epsilon^{1/3}, -18p_\epsilon^{2/3})$, where $|p_\epsilon| \equiv |e^{2\pi i\tau}| \ll 1$ and (y_1, y_2, y_3) is given in Appendix A. Then, the Majorana mass matrix in Eq. (I.3) is rewritten by

$$M_N \approx M_0 \begin{bmatrix} 2(1 + 12p_\epsilon) & 18p_\epsilon^{2/3} & 6p_\epsilon^{1/3} \\ 18p_\epsilon^{2/3} & -12p_\epsilon^{1/3} & -(1 + 12p_\epsilon) \\ 6p_\epsilon^{1/3} & -(1 + 12p_\epsilon) & -36p_\epsilon^{2/3} \end{bmatrix}. \quad (\text{II.1})$$

It is diagonalized by a unitary matrix U_N as $D \equiv U_N^* M_N U_N^\dagger$, and their mass eigenstates are defined by ψ , where $N = U_N^\dagger \psi$. Therefore, $|D|^2 = U_N M_N^\dagger M_N U_N^\dagger$. Approximately U_N and $|D|$ are given by the following forms:

$$U_N \approx \begin{bmatrix} -3\sqrt{2}p_\epsilon^{1/3}(1 - 6p_\epsilon^{1/3}) & -\frac{1}{\sqrt{2}}(1 - 3\epsilon^{1/3} + \frac{9}{2}p_\epsilon^{2/3}) & \frac{1}{\sqrt{2}}(1 + 3\epsilon^{1/3} - \frac{63}{2}p_\epsilon^{2/3}) \\ -\sqrt{2}p_\epsilon^{1/3}(1 - 2p_\epsilon^{1/3}) & \frac{1}{\sqrt{2}}(1 + 3\epsilon^{1/3} - \frac{35}{2}p_\epsilon^{2/3}) & \frac{1}{\sqrt{2}}(1 - 3\epsilon^{1/3} + \frac{13}{2}p_\epsilon^{2/3}) \\ 1 - 10p_\epsilon^{1/3} & -2p_\epsilon^{1/3}(1 - 14p_\epsilon^{1/3}) & 2p_\epsilon^{1/3}(2 - 7p_\epsilon^{1/3}) \end{bmatrix}^* + \mathcal{O}(p_\epsilon), \quad (\text{II.2})$$

$$|D| \approx M_0 \text{diag.} [1 - 6p_\epsilon^{1/3} - 18p_\epsilon^{2/3}, 1 + 6p_\epsilon^{1/3} + 42p_\epsilon^{2/3}, 2 + 24p_\epsilon^{2/3}] + \mathcal{O}(p_\epsilon). \quad (\text{II.3})$$

Thus, one can straightforwardly find that $|D| = M_0 \text{diag.}[1, 1, 2]$ in the limit of $\tau \rightarrow i\infty$.

B. Inert scalar boson mass matrices

Inert scalar boson components of $\hat{\eta}_{1,2}$ and $\hat{\chi}$ contribute to the neutrino mass matrix. The relevant Lagrangian among these bosons is given via soft SUSY-breaking terms as follows:

$$-\mathcal{L}_{\text{soft}} = m_A H_2 \eta_1 \chi + m_B^2 \chi^2 + m_{\eta_1}^2 |\eta_1|^2 + m_\chi^2 |\chi|^2 \quad (\text{II.4})$$

$$+ m_{H_1}^2 |H_1|^2 + m_{H_2}^2 |H_2|^2 + m_{\eta_2}^2 |\eta_2|^2 + \mu_{BH}^2 H_1 H_2 + \mu_{B\eta}^2 \eta_1 \eta_2 + m'_A H_1 \eta_2 \chi + \text{h.c.},$$

where the terms in the first line of RHS directly contributes to the neutrino mass matrix and some of mass parameters include modular forms. When the neutral components are written in terms of real and imaginary part as $\chi = (\chi_R + i\chi_I)/\sqrt{2}$ and $\eta_1 = (\eta_1^+, (\eta_{R_1} + i\eta_{I_1})/\sqrt{2})^T$, the mass squared matrices in basis of $(\eta_1, \chi)_{R,I}$ are given by

$$m_{R,I}^2 = \begin{bmatrix} m_{\eta_1}^2 & \frac{v_2 m_A}{\sqrt{2}} \\ \frac{v_2 m_A}{\sqrt{2}} & m_\chi^2 + m_B^2 \end{bmatrix}, \quad m_I^2 = \begin{bmatrix} m_{\eta_1}^2 & -\frac{v_2 m_A}{\sqrt{2}} \\ -\frac{v_2 m_A}{\sqrt{2}} & m_\chi^2 - m_B^2 \end{bmatrix}, \quad (\text{II.5})$$

these are diagonalized by $D_{R,I}^2 = O_{R,I} M_{R,I}^2 O_{R,I}^T$, where $O_{R,I}$ is an orthogonal matrix;

$$\begin{bmatrix} \eta_1 \\ \chi \end{bmatrix}_{R,I} = \begin{bmatrix} c_{R,I} & s_{R,I} \\ -s_{R,I} & c_{R,I} \end{bmatrix} \begin{bmatrix} \varphi_1 \\ \varphi_2 \end{bmatrix}_{R,I}, \quad O_{R,I} = \begin{bmatrix} c_{R,I} & s_{R,I} \\ -s_{R,I} & c_{R,I} \end{bmatrix}. \quad (\text{II.6})$$

Here $\varphi_{1R,2R,1I,2I}$ are mass eigenvectors, $s_{R,I}$, $c_{R,I}$ are respectively short-hand notations for $\sin \theta_{R,I}$, $\cos \theta_{R,I}$ which are given by a function of mass parameters in Eq. (II.5).

C. Neutrino sector

Now we can discuss the neutrino sector estimating neutrino mass at one-loop level. Our valid renormalizable Lagrangian in terms of mass eigenstates of heavier Majorana fermions and inert scalar bosons, coming from superpotential, is given by

$$-\mathcal{L}^\nu = \frac{1}{\sqrt{2}} \bar{\psi}_i (U_N)_{ia} y_{\eta_{ab}} \nu_b (c_R \varphi_{1R} + s_R \varphi_{2R}) + \frac{i}{\sqrt{2}} \bar{\psi}_i (U_N)_{ia} y_{\eta_{ab}} \nu_b (c_I \varphi_{1I} + s_I \varphi_{2I}) + \text{h.c.}, \quad (\text{II.7})$$

$$y_\eta = \begin{bmatrix} a_\eta & 0 & 0 \\ 0 & b_\eta & 0 \\ 0 & 0 & c_\eta \end{bmatrix} \begin{bmatrix} y_1^{(6)} + \epsilon_e y_1'^{(6)} & y_3^{(6)} + \epsilon_e y_3'^{(6)} & y_2^{(6)} + \epsilon_e y_2'^{(6)} \\ y_3^{(6)} + \epsilon_\mu y_3'^{(6)} & y_2^{(6)} + \epsilon_\mu y_2'^{(6)} & y_1^{(6)} + \epsilon_\mu y_1'^{(6)} \\ y_2^{(4)} & y_1^{(4)} & y_3^{(4)} \end{bmatrix}, \quad (\text{II.8})$$

where a_η , b_η , c_η are real without loss of generality after phase redefinition, while $\epsilon_{e,\mu}$ are complex values which would also be sources of CP asymmetry in addition to τ . Explicit forms of $(y_1^{(4)}, y_2^{(4)}, y_3^{(4)})$, $(y_1^{(6)}, y_2^{(6)}, y_3^{(6)})$, and $(y_1'^{(6)}, y_2'^{(6)}, y_3'^{(6)})$ are given in Appendix A. Then, the neutrino mass matrix is given as follows:

$$(m_\nu)_{ab} = -\frac{1}{2(4\pi)^2} (y_\eta)_{a\beta}^T (U_N^T)_{\beta i} D_i (U_N)_{i\alpha} (y_\eta)_{\alpha b} \\ \times [c_R^2 F(m_{\varphi_{1R}}, D_i) - c_I^2 F(m_{\varphi_{1I}}, D_i) + s_R^2 F(m_{\varphi_{2R}}, D_i) - s_I^2 F(m_{\varphi_{2I}}, D_i)], \quad (\text{II.9})$$

where

$$F(m_a, m_b) = \frac{\ln\left(\frac{m_a^2}{m_b^2}\right)}{\frac{m_a^2}{m_b^2} - 1} - 1. \quad (\text{II.10})$$

The neutrino mass matrix m_ν is then diagonalized by an unitary matrix U_{PMNS} ; $U_{\text{PMNS}}^T m_\nu U_{\text{PMNS}} \equiv \text{diag}(m_1, m_2, m_3)$. We write two mass squared differences measured by the experiments,

$$\Delta m_{\text{sol}}^2 = m_2^2 - m_1^2, \quad (\text{II.11})$$

$$(\text{NH}) : \Delta m_{\text{atm}}^2 = m_3^2 - m_1^2, \quad (\text{IH}) : \Delta m_{\text{atm}}^2 = m_2^2 - m_3^2, \quad (\text{II.12})$$

where Δm_{sol}^2 is solar mass squared difference and Δm_{atm}^2 is atmospheric neutrino mass squared difference whose form depends on whether neutrino mass ordering is normal hierarchy (NH) or inverted hierarchy (IH). U_{PMNS} is parametrized by three mixing angle θ_{ij} ($i, j = 1, 2, 3; i < j$), one CP violating Dirac phase δ_{CP} , and two Majorana phases $\{\alpha_{21}, \alpha_{32}\}$ as follows:

$$U_{\text{PMNS}} = \begin{pmatrix} c_{12}c_{13} & s_{12}c_{13} & s_{13}e^{-i\delta_{CP}} \\ -s_{12}c_{23} - c_{12}s_{23}s_{13}e^{i\delta_{CP}} & c_{12}c_{23} - s_{12}s_{23}s_{13}e^{i\delta_{CP}} & s_{23}c_{13} \\ s_{12}s_{23} - c_{12}c_{23}s_{13}e^{i\delta_{CP}} & -c_{12}s_{23} - s_{12}c_{23}s_{13}e^{i\delta_{CP}} & c_{23}c_{13} \end{pmatrix} \begin{pmatrix} 1 & 0 & 0 \\ 0 & e^{i\frac{\alpha_{21}}{2}} & 0 \\ 0 & 0 & e^{i\frac{\alpha_{31}}{2}} \end{pmatrix}, \quad (\text{II.13})$$

where c_{ij} and s_{ij} stands for $\cos \theta_{ij}$ and $\sin \theta_{ij}$ respectively. Then, each mixing angle is given in terms of the component of U_{PMNS} as follows:

$$\sin^2 \theta_{13} = |(U_{\text{PMNS}})_{13}|^2, \quad \sin^2 \theta_{23} = \frac{|(U_{\text{PMNS}})_{23}|^2}{1 - |(U_{\text{PMNS}})_{13}|^2}, \quad \sin^2 \theta_{12} = \frac{|(U_{\text{PMNS}})_{12}|^2}{1 - |(U_{\text{PMNS}})_{13}|^2}. \quad (\text{II.14})$$

Also, we compute the Jarlskog invariant, δ_{CP} derived from PMNS matrix elements $U_{\alpha i}$:

$$J_{CP} = \text{Im}[U_{e1}U_{\mu 2}U_{e2}^*U_{\mu 1}^*] = s_{23}c_{23}s_{12}c_{12}s_{13}c_{13}^2 \sin \delta_{CP}, \quad (\text{II.15})$$

and the Majorana phases are also estimated in terms of other invariants I_1 and I_2 :

$$I_1 = \text{Im}[U_{e1}^*U_{e2}] = c_{12}s_{12}c_{13}^2 \sin\left(\frac{\alpha_{21}}{2}\right), \quad I_2 = \text{Im}[U_{e1}^*U_{e3}] = c_{12}s_{13}c_{13} \sin\left(\frac{\alpha_{31}}{2} - \delta_{CP}\right). \quad (\text{II.16})$$

Additionally, the effective mass for the neutrinoless double beta decay is given by

$$\langle m_{ee} \rangle = |m_1 \cos^2 \theta_{12} \cos^2 \theta_{13} + m_2 \sin^2 \theta_{12} \cos^2 \theta_{13} e^{i\alpha_{21}} + m_3 \sin^2 \theta_{13} e^{i(\alpha_{31} - 2\delta_{CP})}|, \quad (\text{II.17})$$

where its observed value could be measured by KamLAND-Zen in future [75]. We will adopt the neutrino experimental data in NuFit5.0 [76] in order to perform the numerical χ^2 analysis.

III. RESONANT LEPTOGENESIS

Now we consider non-thermal leptogenesis where population of the lightest sterile neutrino increases as the temperature decreases, so-called freeze-in production. The generation of the lepton asymmetry is non-equilibrium decay process of the lightest neutrino ψ_1 . The dominant contribution to the CP asymmetry is arisen from the interference between tree and one-loop diagrams for decays of ψ_1 via Yukawa coupling y_η . In general, there are two one-loop decay modes; vertex correction diagram and self-energy correction, but the self energy correction is dominant in our case since ψ_1 and ψ_2 have degenerate mass. Hence, the main source of CP asymmetry ϵ_1 is approximately given as follows:

$$\epsilon_1 \approx \frac{\text{Im}(h^\dagger h)_{12}^2}{(h^\dagger h)_{11}^2 (h^\dagger h)_{22}^2} \frac{(D_1^2 - D_2^2) D_1 \Gamma_2}{(D_1^2 - D_2^2)^2 + D_1^2 \Gamma_{\psi_2}^2}, \quad (\text{III.1})$$

$$\Gamma_{\psi_2} = \frac{|h_{2i}|^2}{4\pi} D_2 \left(1 - \frac{m_{\eta_1}^2}{D_2^2}\right)^2, \quad (\text{III.2})$$

where $h \equiv U_N y_\eta$, and we expect $m_{\eta_1} \approx m_{\varphi_{1R}} \approx m_{\varphi_{1I}}$. Then, we obtain the lepton asymmetry by solving the approximated Boltzmann equations for ψ_1 and lepton number densities as

follows:

$$\frac{dY_{\psi_1}}{dz} \approx -\frac{z}{sH(D_1)} \left(\frac{Y_{\psi_1}}{Y_{\psi_1}^{eq}} - 1 \right) \gamma_D^{\psi_1}, \quad (\text{III.3})$$

$$\frac{dY_L}{dz} \approx \frac{z}{sH(D_1)} \left(\frac{Y_{\psi_1}}{Y_{\psi_1}^{eq}} - 1 \right) \epsilon_1 \gamma_D^{\psi_1}, \quad (\text{III.4})$$

$$\gamma_D^{\psi_1} = \sum_{i=1}^3 \frac{|h_{1i}|^2}{4\pi^3} D_1^4 \left(1 - \frac{m_{\eta_1}^2}{D_1^2} \right)^2 \frac{K_1(z)}{z}, \quad (\text{III.5})$$

where $z \equiv D_1/T$, T being temperature, $H(D_1) = 1.66g_*^{1/2}D_1^2/M_{pl}$, $g_* \approx 100$ is the number of relativistic degrees of freedom, and Plank mass $M_{pl} \approx 1.2 \times 10^{19}$ GeV. We denote the entropy density as $Y_{\psi_1} \equiv n_{\psi_1}/s$ and $Y_L \equiv (n_L - n_{\bar{L}})/s$, $s = 2\pi^2 g_* T^3/45$. Furthermore, $Y_{\psi_1}^{eq}$ is given by $45z^2 K_2(z)/(2\pi^4 g_*)$, $K_{1(2)}(z)$, where the modified Bessel function of the first(second) kind. Once the lepton asymmetry Y_L is generated, it is converted by $B + L$ violating spharelon transitions [77, 78]. Then, the conversion rate is straightforwardly derived by the chemical equilibrium conditions and it is found as

$$Y_B = -\frac{8}{23} Y_L(z_{EW}), \quad (\text{III.6})$$

where z_{EW} corresponds to the spharelon decoupling temperature and we set to be $T_{EW} = 100$ GeV. Here, we should mention scattering processes that should be included in the above Boltzmann equations in general, since these processes also change the number of lepton as well as ψ . The lepton number is changed by the processes of $\ell\ell \rightarrow \eta\eta$ and $\eta\ell \rightarrow \eta^\dagger\bar{\ell}$, and the change of ψ_1 number is caused by $\psi_1\psi_1 \rightarrow \ell\bar{\ell}$ and $\psi_1\psi_1 \rightarrow \eta\eta^\dagger$ [73]. Even though there exist resonant enhancement, the wash out processes from these scattering processes could be dominant depending on the parameter region. In order to suppress these processes enough, we should work on, e.g., $D_1 \lesssim 2.5$ TeV when $|h| \approx 10^{-4}$ ⁶. Otherwise, we have to include the scattering processes. In our numerical analysis, we compute the simplified Boltzmann equations by carefully checking whether the washout processes can be neglected or not for our allowed parameter sets from neutrino data fitting. In addition, the number density of N_1 is generated by freeze-in mechanism and it becomes the same order as that of thermal equilibrium for temperature higher than electroweak scale.

⁶ The order 10^{-4} comes from a prior research in ref. [73]. In this situation, LFVs are suppressed enough to satisfy the current experiments. In fact, the stringent constraint of $\mu \rightarrow e\gamma$ gives 4.2×10^{-13} of the branching ratio, while our maximum value of this process is 10^{-16} at most in our numerical analysis. Thus, we do not mention LFVs furthermore.

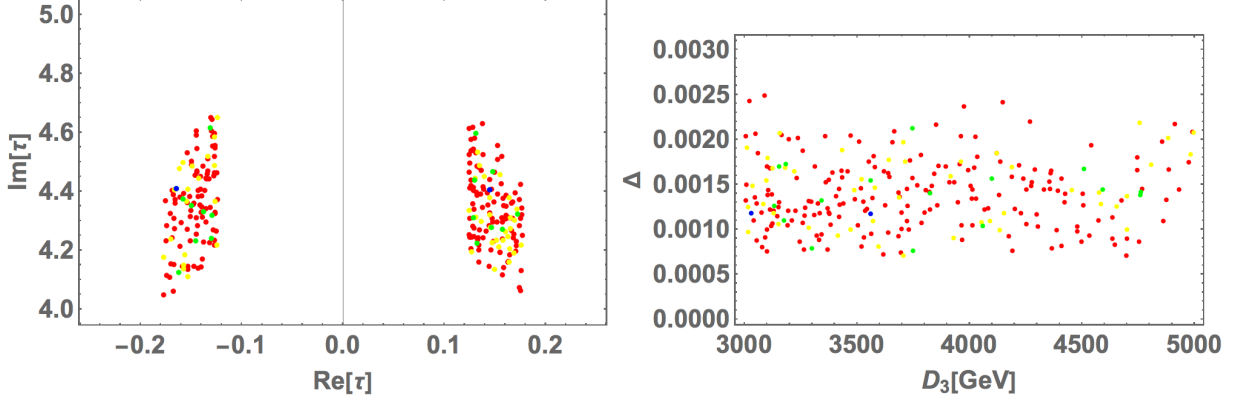


FIG. 1: The left plot shows allowed region of τ , while the right one shows the mass degeneracy of D_1 and D_2 that is defined by $\Delta \equiv (D_2 - D_1)/D_2$ in terms of D_3 in GeV unit, where $D_2(\sim D_1) \sim D_3/2$. Each point in blue, green, yellow, and red color represents the allowed region in $\sigma \leq 1$, $1 < \sigma \leq 2$, $2 < \sigma \leq 3$, and $3 < \sigma \leq 5$ interval, respectively.

IV. NUMERICAL ANALYSIS

In this section, we carry out numerical analysis searching for allowed parameter region satisfying phenomenological constraints. *Note first that we find there is no allowed regions simultaneously satisfying the observed neutrino oscillation data and BAU in case of IH. Thus, we focus on the case of NH only.* We show the allowed region with χ^2 analysis in the lepton sector, where we randomly select the values of input parameters within the following ranges,

$$\begin{aligned}
 |\text{Re}(\tau)| &\in [10^{-3}, 0.5], \quad \text{Im}(\tau) \in [2, 10], \quad \{a_\eta, b_\eta, c_\eta\} \in [10^{-8}, 10^{-3}], \quad \{|\epsilon_e|, |\epsilon_\mu|\} \in [10^{-3}, 10^3] \\
 M_0 &\in [10^2, 10^5] \text{ GeV}, \quad m_{\eta_1} \in [70, 10^3] \text{ GeV}, \quad m_\chi \in [1, 10^3] \text{ GeV}, \quad \{m_A, m_B\} \in [0.001, 50] \text{ GeV},
 \end{aligned}
 \tag{IV.1}$$

where we expect the source of CP asymmetry arises from three complex values τ , ϵ_e , ϵ_μ . We also require inert scalar bosons are lighter than ψ_1 so that ψ_1 can decay into scalar boson and lepton to realize leptogenesis. Then, we accumulate the data if five measured neutrino oscillation data; $(\Delta m_{\text{atm}}^2, \Delta m_{\text{sol}}^2, \sin^2 \theta_{13}, \sin^2 \theta_{23}, \sin^2 \theta_{12})$ [76] and BAU in Eq. (I.2) are satisfied at the same time. Notice here that we regard δ_{CP} as a predicted value due to large ambiguity of experimental result in 3σ interval.

The left plot of Fig. 1 shows allowed region of τ , while the right one shows the mass

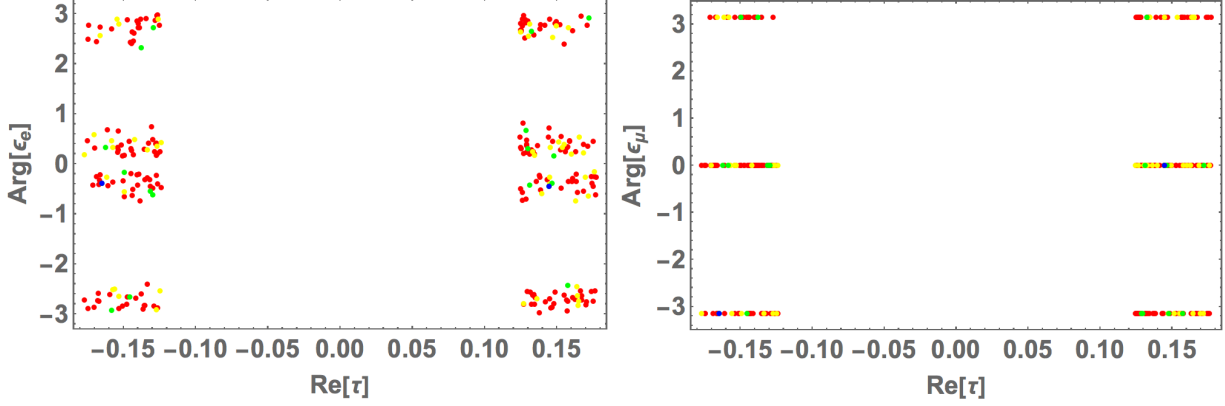


FIG. 2: The left(right) plot shows allowed region of $\text{Arg}[\epsilon_{e(\mu)}]$ in terms of $\text{Re}[\tau]$, where the color legends are the same as the one in Fig. 1.

degeneracy of D_1 and D_2 that is defined by $\Delta \equiv (D_2 - D_1)/D_2$ in terms of D_3 in GeV unit, where $D_2(\sim D_1) \sim D_3/2$. Each point in blue, green, yellow, and red color represents the allowed region in $\sigma \leq 1$, $1 < \sigma \leq 2$, $2 < \sigma \leq 3$, and $3 < \sigma \leq 5$ interval, respectively. These figures suggest that $0.12 \lesssim \text{Re}|\tau| \lesssim 0.18$ and $4.05 \lesssim \text{Im}[\tau] \lesssim 4.65$, $7 \times 10^{-4} \lesssim \Delta \lesssim 2.5 \times 10^{-3}$, and $3000 \text{ GeV} \lesssim D_3 \lesssim 5000 \text{ GeV}$. Note here that the smaller Δ directly corresponds to the larger imaginary part of τ , while the $\text{Re}[\tau]$ plays a role in generating one of the CP sources together with $\epsilon_{e,\mu}$. We thus find sizable $\text{Re}[\tau]$ value is required in our allowed region and it suggests that *the main source of CP asymmetry would arise from τ* .

In order to investigate the main source of CP asymmetry, we demonstrate the plots of arguments of $\epsilon_{e,\mu}$ in terms of $\text{Re}[\tau]$ in Fig. 2, where the color legends are the same as the one in Fig. 1. Remarkably, argument of ϵ_μ is almost zero while the one of ϵ_e is slightly deviated from zero. It comes from the resonant leptogenesis and neutrino oscillation. In order to achieve the resonant leptogenesis, we need $(y_1, y_2, y_3) \sim (1, 0, 0)$. It implies that $(y_1^{(6)}, y_2^{(6)}, y_3^{(6)}) \sim (1, 0, 0)$ and $(y_1'^{(6)}, y_2'^{(6)}, y_3'^{(6)}) \sim (0, 0, 0)$, leading y_η to

$$y_\eta \sim \begin{bmatrix} 1 & 0 & 0 \\ 0 & 0 & 1 \\ 0 & 1 & 0 \end{bmatrix}. \quad (\text{IV.2})$$

On the other hand, $y_{\eta_{12,13}} \ll y_{\eta_{21,32}}$ are required in order to obtain the observable neutrino oscillation data. In order to compensate the tiny components of $Y_3^{(6)}, Y_{3'}^{(6)}$, rather large value of $\text{Re}[\epsilon_\mu]$ is needed. Thus, the argument of ϵ_μ is relatively tiny. Since both the arguments

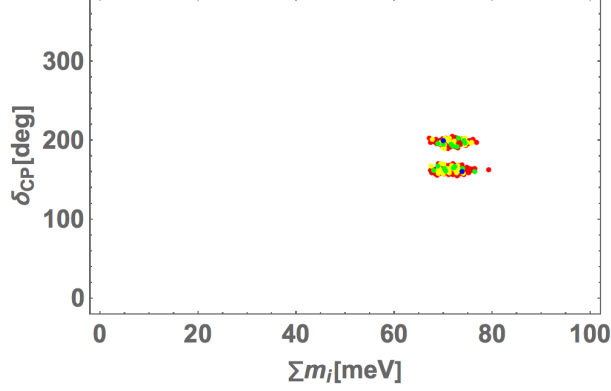


FIG. 3: Allowed region of δ_{CP} in terms of $\sum m_i$, where the color legends are the same as the one in Fig. 1.

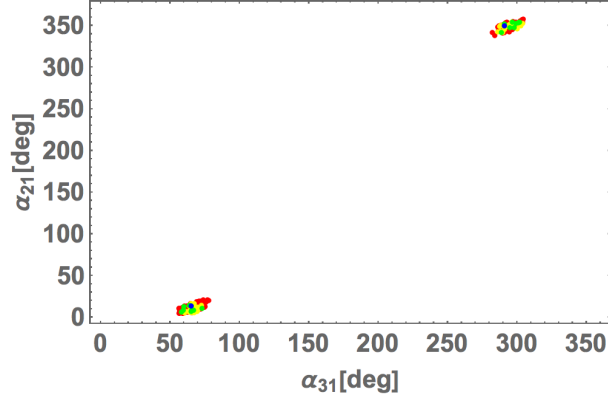


FIG. 4: Allowed region of Majorana phases α_{21} and α_{31} , where the color legends are the same as the one in Fig. 1.

of $\epsilon_{e,\mu}$ are localized at nearby 0 and π , *the main origin of CP asymmetry indeed originates from τ .*

The Fig. 3 shows the allowed region of δ_{CP} in terms of $\sum m_i$, where the color legends are the same as the one in Fig. 1. We find two small localized regions of $150^\circ \lesssim \delta_{\text{CP}} \lesssim 170^\circ$ and $180^\circ \lesssim \delta_{\text{CP}} \lesssim 200^\circ$ with $65 \text{ meV} \lesssim \sum m_i \lesssim 80 \text{ meV}$, where the up island corresponds to the region of $\text{Re}[\tau] < 0$ while the down one corresponds to the region of $\text{Re}[\tau] > 0$. *Our result would favor the best fit value of $\delta_{\text{CP}} = 195^\circ$.*

The Fig. 4 shows Majorana phases α_{21} and α_{31} , where the color legends are the same as the one in Fig. 1. We have two localized islands of $10^\circ \lesssim \alpha_{21} \lesssim 30^\circ$, $55^\circ \lesssim \alpha_{31} \lesssim 80^\circ$, and

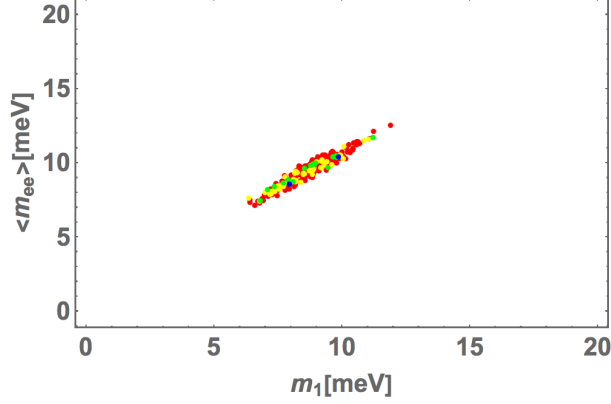


FIG. 5: Allowed region of $\langle m_{ee} \rangle$ in terms of the lightest neutrino mass m_1 meV, where the color legends are the same as the one in Fig. 1.

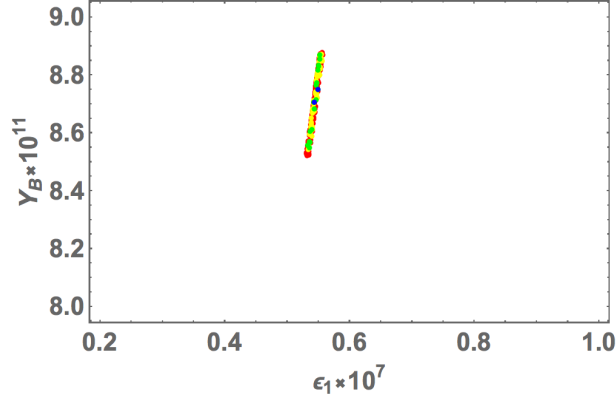


FIG. 6: Allowed region of the baryon asymmetry Y_B in terms of the CP asymmetry source ϵ_1 , where the color legends are the same as the one in Fig. 1 and the Y_B is taken within the observed range in Eq.(I.2).

$330^\circ \lesssim \alpha_{21} \lesssim 360^\circ$, $280^\circ \lesssim \alpha_{31} \lesssim 310^\circ$, where the up-right island corresponds to the region of $\text{Re}[\tau] < 0$ while the down-left one corresponds to the region of $\text{Re}[\tau] > 0$.

The Fig. 5 shows $\langle m_{ee} \rangle$ in terms of the lightest neutrino mass m_1 meV, where the color legends are the same as the one in Fig. 1. We obtain $7 \text{ meV} \lesssim \langle m_{ee} \rangle \lesssim 12 \text{ meV}$ and $6 \text{ meV} \lesssim m_1 \lesssim 13 \text{ meV}$.

We show the baryon asymmetry Y_B in terms of the CP asymmetry source ϵ_1 in Fig. 6, where the color legends are the same as the one in Fig. 1 and the Y_B is taken within the observed range in Eq.(I.2). Here, ϵ_1 is about 5×10^{-8} that is favored by the prior analysis

in Ref. [73]. Finally, we show a benchmark point for NH in Table II that provide minimum $\sqrt{\chi^2}$ in our numerical analysis.

	NH
τ	$-0.165 + 4.41i$
$[a_\eta, b_\eta, c_\eta] \times 10^5$	$[-4.94, -8.42, 6.71]$
$[M_0, M_{\eta_1}, m_\chi]/\text{GeV}$	$[1780, 199, 70.9]$
$[(v_2 m_A/\sqrt{2})^{1/2}, m_B]/\text{GeV}$	$[45.1, 0.0324]$
$[\epsilon_e, \epsilon_\mu]$	$[24.0 - 9.80i, -761 - 0.00522i]$
Δm_{atm}^2	$2.47 \times 10^{-3} \text{eV}^2$
Δm_{sol}^2	$7.37 \times 10^{-5} \text{eV}^2$
$\sin \theta_{12}$	0.544
$\sin \theta_{23}$	0.743
$\sin \theta_{13}$	0.151
$[\delta_{CP}^\ell, \alpha_{21}, \alpha_{31}]$	$[200^\circ, 349^\circ, 291^\circ]$
$\sum m_i$	70 meV
$\langle m_{ee} \rangle$	8.58 meV
ϵ_1	5.43×10^{-8}
Y_B	8.71×10^{-11}
$\sqrt{\Delta\chi^2}$	1.90

TABLE II: Numerical benchmark point of our input parameters and observables at nearby the fixed point $\tau = i \times \infty$ in NH. Here, we take BP so that δ_{CP} is closest to the BF value of 195° within $\sqrt{\Delta\chi^2} \leq 1$.

V. CONCLUSION AND DISCUSSION

We explore a modular A_4 invariant radiative seesaw model. In this model, we can generate the measured baryon asymmetry via resonant leptogenesis as well as the observed neutrino oscillation data. Larger $\text{Im}[\tau]$ leads to the more degenerate Majorana masses. This degenerate masses are preferred by the resonant leptogenesis since larger $\text{Im}[\tau]$ can enhance the CP asymmetry and avoid the washout processes even though keeping the small Yukawa

couplings. While the nonzero $\text{Re}[\tau]$ provides the source of CP asymmetry in addition to free complex parameters. In our case, especially, $\text{Re}[\tau]$ is main source of the CP asymmetry by our χ^2 numerical analysis that would be interesting result in this scenario. Since the constraint of BAU in Eq. (I.2) is very strict, we have obtained narrow allowed region as we have discussed in the numerical analysis. Below, we have highlightend several remarks on the neutrino sector,

1. We have obtained two small localized regions of $150^\circ \lesssim \delta_{\text{CP}} \lesssim 170^\circ$ and $180^\circ \lesssim \delta_{\text{CP}} \lesssim 200^\circ$ with $65 \text{ meV} \lesssim \sum m_i \lesssim 80 \text{ meV}$, where $180^\circ \lesssim \delta_{\text{CP}} \lesssim 200^\circ$ corresponds to the region of $\text{Re}[\tau] < 0$ while $150^\circ \lesssim \delta_{\text{CP}} \lesssim 170^\circ$ corresponds to the region of $\text{Re}[\tau] > 0$. *Our result would favor the best fit value of $\delta_{\text{CP}} = 195^\circ$.*
2. We have found two localized islands of $10^\circ \lesssim \alpha_{21} \lesssim 30^\circ$, $55^\circ \lesssim \alpha_{31} \lesssim 80^\circ$, and $330^\circ \lesssim \alpha_{21} \lesssim 360^\circ$, $280^\circ \lesssim \alpha_{31} \lesssim 310^\circ$, where $330^\circ \lesssim \alpha_{21} \lesssim 360^\circ$, $280^\circ \lesssim \alpha_{31} \lesssim 310^\circ$ corresponds to the region of $\text{Re}[\tau] < 0$ while $10^\circ \lesssim \alpha_{21} \lesssim 30^\circ$, $55^\circ \lesssim \alpha_{31} \lesssim 80^\circ$ one corresponds to the region of $\text{Re}[\tau] > 0$.
3. We have gotten $7 \text{ meV} \lesssim \langle m_{ee} \rangle \lesssim 12 \text{ meV}$ and $6 \text{ meV} \lesssim m_1 \lesssim 13 \text{ meV}$.

Furthermore, our heavy neutrino masses and inert scalar bosons are order of several hundred GeV to $\mathcal{O}(\text{TeV})$ scale. We thus expect that our model can be tested at collider experiments such as the LHC. For example, inert scalar bosons from doublet can be produced via electroweak interactions. Detailed collider analysis is beyond the scope of this paper and it will be done in future work.

Acknowledgments

This work is in part supported by KIAS Individual Grants, Grant No. PG074202 (JK) and Grant No. PG076202 (DWK) at Korea Institute for Advanced Study. This research was supported by an appointment to the JRG Program at the APCTP through the Science and Technology Promotion Fund and Lottery Fund of the Korean Government. This was also supported by the Korean Local Governments - Gyeongsangbuk-do Province and Pohang City (H.O.). H. O. is sincerely grateful for the KIAS member, and log cabin at POSTECH

to provide nice space to come up with this project. The work was also supported by the Fundamental Research Funds for the Central Universities (T. N.).

Appendix A: Formulas in modular A_4 framework

Here we summarize some formulas of A_4 modular symmetry framework. Modular forms are holomorphic functions of modulus τ , $f(\tau)$, which are transformed by

$$\tau \longrightarrow \gamma\tau = \frac{a\tau + b}{c\tau + d}, \quad \text{where } a, b, c, d \in \mathbb{Z} \text{ and } ad - bc = 1, \quad \text{Im}[\tau] > 0, \quad (\text{A.1})$$

$$f(\gamma\tau) = (c\tau + d)^k f(\tau), \quad \gamma \in \Gamma(N), \quad (\text{A.2})$$

where k is the so-called as the modular weight.

A superfield $\phi^{(I)}$ is transformed under the modular transformation as

$$\phi^{(I)} \rightarrow (c\tau + d)^{-k_I} \rho^{(I)}(\gamma) \phi^{(I)}, \quad (\text{A.3})$$

where $-k_I$ is the modular weight and $\rho^{(I)}(\gamma)$ represents an unitary representation matrix corresponding to A_4 transformation. Thus superpotential is invariant if sum of modular weight from fields and modular form in corresponding term is zero (also it should be invariant under A_4 and gauge symmetry).

The basis of modular forms is weight 2, $Y_3^{(2)} = (y_1, y_2, y_3)$, transforming as a triplet of A_4 that is written in terms of the Dedekind eta-function $\eta(\tau)$ and its derivative [10]:

$$\begin{aligned} y_1(\tau) &= \frac{i}{2\pi} \left(\frac{\eta'(\tau/3)}{\eta(\tau/3)} + \frac{\eta'((\tau+1)/3)}{\eta((\tau+1)/3)} + \frac{\eta'((\tau+2)/3)}{\eta((\tau+2)/3)} - \frac{27\eta'(3\tau)}{\eta(3\tau)} \right), \\ y_2(\tau) &= \frac{-i}{\pi} \left(\frac{\eta'(\tau/3)}{\eta(\tau/3)} + \omega^2 \frac{\eta'((\tau+1)/3)}{\eta((\tau+1)/3)} + \omega \frac{\eta'((\tau+2)/3)}{\eta((\tau+2)/3)} \right), \\ y_3(\tau) &= \frac{-i}{\pi} \left(\frac{\eta'(\tau/3)}{\eta(\tau/3)} + \omega \frac{\eta'((\tau+1)/3)}{\eta((\tau+1)/3)} + \omega^2 \frac{\eta'((\tau+2)/3)}{\eta((\tau+2)/3)} \right), \\ \eta(\tau) &= q^{1/24} \prod_{n=1}^{\infty} (1 - q^n), \quad q = e^{2\pi i \tau}, \quad \omega = e^{2\pi i/3}. \end{aligned} \quad (\text{A.4})$$

Modular forms with higher weight can be obtained from $y_{1,2,3}(\tau)$ through the A_4 multiplication rules as shown the last part. Thus, some A_4 triplet modular forms used in our analysis are derived as follows:

$$Y_3^{(4)} \equiv (y_1^{(4)}, y_2^{(4)}, y_3^{(4)}) = (y_1^2 - y_2 y_3, y_3^2 - y_1 y_2, y_2^2 - y_1 y_3), \quad (\text{A.5})$$

$$Y_3^{(6)} \equiv (y_1^{(6)}, y_2^{(6)}, y_3^{(6)}) = (y_1^3 + 2y_1 y_2 y_3, y_2^2 y_2 + 2y_2^2 y_3, y_1^2 y_3 + 2y_3^2 y_2), \quad (\text{A.6})$$

$$Y_{3'}^{(6)} \equiv (y_1'^{(6)}, y_2'^{(6)}, y_3'^{(6)}) = (y_3^3 + 2y_1 y_2 y_3, y_3^2 y_1 + 2y_1^2 y_2, y_3^2 y_2 + 2y_2^2 y_1). \quad (\text{A.7})$$

A_4 multiplication rules are given by

$$\begin{aligned}
\begin{pmatrix} a_1 \\ a_2 \\ a_3 \end{pmatrix}_{\mathbf{3}} \otimes \begin{pmatrix} b_1 \\ b_2 \\ b_3 \end{pmatrix}_{\mathbf{3}'} &= (a_1 b_1 + a_2 b_3 + a_3 b_2)_{\mathbf{1}} \oplus (a_3 b_3 + a_1 b_2 + a_2 b_1)_{\mathbf{1}'} \\
&\oplus (a_2 b_2 + a_1 b_3 + a_3 b_1)_{\mathbf{1}''} \\
&\oplus \frac{1}{3} \begin{pmatrix} 2a_1 b_1 - a_2 b_3 - a_3 b_2 \\ 2a_3 b_3 - a_1 b_2 - a_2 b_1 \\ 2a_2 b_2 - a_1 b_3 - a_3 b_1 \end{pmatrix}_{\mathbf{3}} \oplus \frac{1}{2} \begin{pmatrix} a_2 b_3 - a_3 b_2 \\ a_1 b_2 - a_2 b_1 \\ a_3 b_1 - a_1 b_3 \end{pmatrix}_{\mathbf{3}'} , \\
a_{1'} \otimes \begin{pmatrix} b_1 \\ b_2 \\ b_3 \end{pmatrix}_{\mathbf{3}} &= a \begin{pmatrix} b_3 \\ b_1 \\ b_2 \end{pmatrix}_{\mathbf{3}} , \quad a_{1''} \otimes \begin{pmatrix} b_1 \\ b_2 \\ b_3 \end{pmatrix}_{\mathbf{3}} = a \begin{pmatrix} b_2 \\ b_3 \\ b_1 \end{pmatrix}_{\mathbf{3}} , \\
\mathbf{1} \otimes \mathbf{1} &= \mathbf{1} , \quad \mathbf{1}' \otimes \mathbf{1}' = \mathbf{1}'' , \quad \mathbf{1}'' \otimes \mathbf{1}'' = \mathbf{1}' , \quad \mathbf{1}' \otimes \mathbf{1}'' = \mathbf{1} .
\end{aligned} \tag{A.8}
\end{aligned}$$

-
- [1] N. Aghanim *et al.* [Planck], *Astron. Astrophys.* **641** (2020), A6 [erratum: *Astron. Astrophys.* **652** (2021), C4] [arXiv:1807.06209 [astro-ph.CO]].
- [2] A. G. Cohen, D. B. Kaplan and A. E. Nelson, *Ann. Rev. Nucl. Part. Sci.* **43** (1993), 27-70 [arXiv:hep-ph/9302210 [hep-ph]].
- [3] K. Y. Choi, S. K. Kang and J. Kim, *Phys. Lett. B* **782**, 657-661 (2018) [arXiv:1803.00820 [hep-ph]].
- [4] M. Fukugita and T. Yanagida, *Phys. Lett. B* **174** (1986), 45-47
- [5] P. Minkowski, *Phys. Lett. B* **67** (1977), 421-428
- [6] R. N. Mohapatra and G. Senjanovic, *Phys. Rev. Lett.* **44** (1980), 912
- [7] A. Pilaftsis and T. E. J. Underwood, *Nucl. Phys. B* **692** (2004), 303-345 [arXiv:hep-ph/0309342 [hep-ph]].
- [8] A. Pilaftsis, *Phys. Rev. D* **56** (1997), 5431-5451 [arXiv:hep-ph/9707235 [hep-ph]].
- [9] M. Flanz, E. A. Paschos, U. Sarkar and J. Weiss, *Phys. Lett. B* **389** (1996), 693-699 [arXiv:hep-ph/9607310 [hep-ph]].
- [10] F. Feruglio, [arXiv:1706.08749 [hep-ph]].

- [11] R. de Adelhart Toorop, F. Feruglio and C. Hagedorn, Nucl. Phys. B **858**, 437-467 (2012) [arXiv:1112.1340 [hep-ph]].
- [12] J. C. Criado and F. Feruglio, SciPost Phys. **5**, no.5, 042 (2018) [arXiv:1807.01125 [hep-ph]].
- [13] T. Kobayashi, N. Omoto, Y. Shimizu, K. Takagi, M. Tanimoto and T. H. Tatsuishi, JHEP **11**, 196 (2018) [arXiv:1808.03012 [hep-ph]].
- [14] H. Okada and M. Tanimoto, Phys. Lett. B **791**, 54-61 (2019) [arXiv:1812.09677 [hep-ph]].
- [15] T. Kobayashi, H. Okada and Y. Orikasa, [arXiv:2111.05674 [hep-ph]].
- [16] T. Nomura and H. Okada, Phys. Lett. B **797**, 134799 (2019) [arXiv:1904.03937 [hep-ph]].
- [17] H. Okada and M. Tanimoto, Eur. Phys. J. C **81**, no.1, 52 (2021) [arXiv:1905.13421 [hep-ph]].
- [18] F. J. de Anda, S. F. King and E. Perdomo, Phys. Rev. D **101**, no.1, 015028 (2020) [arXiv:1812.05620 [hep-ph]].
- [19] P. P. Novichkov, S. T. Petcov and M. Tanimoto, Phys. Lett. B **793**, 247-258 (2019) [arXiv:1812.11289 [hep-ph]].
- [20] T. Nomura and H. Okada, Nucl. Phys. B **966**, 115372 (2021) [arXiv:1906.03927 [hep-ph]].
- [21] H. Okada and Y. Orikasa, [arXiv:1907.13520 [hep-ph]].
- [22] G. J. Ding, S. F. King and X. G. Liu, JHEP **09**, 074 (2019) [arXiv:1907.11714 [hep-ph]].
- [23] T. Kobayashi, Y. Shimizu, K. Takagi, M. Tanimoto and T. H. Tatsuishi, Phys. Rev. D **100**, no.11, 115045 (2019) [erratum: Phys. Rev. D **101**, no.3, 039904 (2020)] [arXiv:1909.05139 [hep-ph]].
- [24] T. Asaka, Y. Heo, T. H. Tatsuishi and T. Yoshida, JHEP **01**, 144 (2020) [arXiv:1909.06520 [hep-ph]].
- [25] D. Zhang, Nucl. Phys. B **952**, 114935 (2020) [arXiv:1910.07869 [hep-ph]].
- [26] G. J. Ding, S. F. King, X. G. Liu and J. N. Lu, JHEP **12**, 030 (2019) [arXiv:1910.03460 [hep-ph]].
- [27] T. Kobayashi, T. Nomura and T. Shimomura, Phys. Rev. D **102**, no.3, 035019 (2020) [arXiv:1912.00637 [hep-ph]].
- [28] T. Nomura, H. Okada and S. Patra, Nucl. Phys. B **967**, 115395 (2021) [arXiv:1912.00379 [hep-ph]].
- [29] X. Wang, Nucl. Phys. B **957**, 115105 (2020) [arXiv:1912.13284 [hep-ph]].
- [30] H. Okada and Y. Shoji, Nucl. Phys. B **961**, 115216 (2020) [arXiv:2003.13219 [hep-ph]].
- [31] H. Okada and M. Tanimoto, [arXiv:2005.00775 [hep-ph]].

- [32] M. K. Behera, S. Singirala, S. Mishra and R. Mohanta, [arXiv:2009.01806 [hep-ph]].
- [33] M. K. Behera, S. Mishra, S. Singirala and R. Mohanta, [arXiv:2007.00545 [hep-ph]].
- [34] T. Nomura and H. Okada, [arXiv:2007.04801 [hep-ph]].
- [35] T. Nomura and H. Okada, [arXiv:2007.15459 [hep-ph]].
- [36] T. Asaka, Y. Heo and T. Yoshida, Phys. Lett. B **811**, 135956 (2020) [arXiv:2009.12120 [hep-ph]].
- [37] H. Okada and M. Tanimoto, Phys. Rev. D **103**, no.1, 015005 (2021) [arXiv:2009.14242 [hep-ph]].
- [38] K. I. Nagao and H. Okada, [arXiv:2010.03348 [hep-ph]].
- [39] H. Okada and M. Tanimoto, JHEP **03**, 010 (2021) [arXiv:2012.01688 [hep-ph]].
- [40] C. Y. Yao, J. N. Lu and G. J. Ding, JHEP **05** (2021), 102 [arXiv:2012.13390 [hep-ph]].
- [41] P. Chen, G. J. Ding and S. F. King, JHEP **04** (2021), 239 [arXiv:2101.12724 [hep-ph]].
- [42] M. Kashav and S. Verma, [arXiv:2103.07207 [hep-ph]].
- [43] H. Okada, Y. Shimizu, M. Tanimoto and T. Yoshida, [arXiv:2105.14292 [hep-ph]].
- [44] I. de Medeiros Varzielas and J. Lourenço, [arXiv:2107.04042 [hep-ph]].
- [45] T. Nomura, H. Okada and Y. Orikasa, [arXiv:2106.12375 [hep-ph]].
- [46] P. T. P. Hutaeruk, D. W. Kang, J. Kim and H. Okada, [arXiv:2012.11156 [hep-ph]].
- [47] G. J. Ding, S. F. King and J. N. Lu, [arXiv:2108.09655 [hep-ph]].
- [48] K. I. Nagao and H. Okada, [arXiv:2108.09984 [hep-ph]].
- [49] Georgianna Charalampous, Stephen F. King, George K. Leontaris, Ye-Ling Zhou [arXiv:2109.11379 [hep-ph]].
- [50] H. Okada and Y. h. Qi, [arXiv:2109.13779 [hep-ph]].
- [51] T. Nomura, H. Okada and Y. h. Qi, [arXiv:2111.10944 [hep-ph]].
- [52] T. Kobayashi, H. Otsuka, M. Tanimoto and K. Yamamoto, [arXiv:2112.00493 [hep-ph]].
- [53] A. Dasgupta, T. Nomura, H. Okada, O. Popov and M. Tanimoto, [arXiv:2111.06898 [hep-ph]].
- [54] X. G. Liu and G. J. Ding, [arXiv:2112.14761 [hep-ph]].
- [55] T. Nomura and H. Okada, [arXiv:2201.10244 [hep-ph]].
- [56] H. Otsuka and H. Okada, [arXiv:2202.10089 [hep-ph]].
- [57] T. Nomura, H. Okada and O. Popov, Phys. Lett. B **803** (2020), 135294 [arXiv:1908.07457 [hep-ph]].
- [58] G. Chauhan, P. S. B. Dev, B. Dziewit, W. Flieger, J. Gluza, K. Grzanka, B. Karmakar,

- J. Vergeest and S. Zieba, [arXiv:2203.08105 [hep-ph]].
- [59] S. Kikuchi, T. Kobayashi, K. Nasu, H. Otsuka, S. Takada and H. Uchida, [arXiv:2203.14667 [hep-ph]].
- [60] T. Kobayashi, H. Otsuka, M. Tanimoto and K. Yamamoto, [arXiv:2204.12325 [hep-ph]].
- [61] J. Gehrlein, S. Petcov, M. Spinrath and A. Titov, [arXiv:2203.06219 [hep-ph]].
- [62] Y. Almumin, M. C. Chen, M. Cheng, V. Knapp-Perez, Y. Li, A. Mondol, S. Ramos-Sanchez, M. Ratz and S. Shukla, [arXiv:2204.08668 [hep-ph]].
- [63] M. Kashav and S. Verma, [arXiv:2205.06545 [hep-ph]].
- [64] G. Altarelli and F. Feruglio, *Rev. Mod. Phys.* **82**, 2701-2729 (2010) [arXiv:1002.0211 [hep-ph]].
- [65] H. Ishimori, T. Kobayashi, H. Ohki, Y. Shimizu, H. Okada and M. Tanimoto, *Prog. Theor. Phys. Suppl.* **183**, 1-163 (2010) [arXiv:1003.3552 [hep-th]].
- [66] H. Ishimori, T. Kobayashi, H. Ohki, H. Okada, Y. Shimizu and M. Tanimoto, *Lect. Notes Phys.* **858**, 1-227 (2012)
- [67] D. Hernandez and A. Y. Smirnov, *Phys. Rev. D* **86**, 053014 (2012) [arXiv:1204.0445 [hep-ph]].
- [68] S. F. King and C. Luhn, *Rept. Prog. Phys.* **76**, 056201 (2013) [arXiv:1301.1340 [hep-ph]].
- [69] S. F. King, A. Merle, S. Morisi, Y. Shimizu and M. Tanimoto, *New J. Phys.* **16**, 045018 (2014) [arXiv:1402.4271 [hep-ph]].
- [70] S. F. King, *Prog. Part. Nucl. Phys.* **94**, 217-256 (2017) [arXiv:1701.04413 [hep-ph]].
- [71] S. T. Petcov, *Eur. Phys. J. C* **78**, no.9, 709 (2018) [arXiv:1711.10806 [hep-ph]].
- [72] T. Kobayashi, H. Ohki, H. Okada, Y. Shimizu and M. Tanimoto,
- [73] S. Kashiwase and D. Suematsu, *Phys. Rev. D* **86** (2012), 053001 [arXiv:1207.2594 [hep-ph]].
- [74] E. Ma, *Phys. Rev. D* **73** (2006), 077301 [arXiv:hep-ph/0601225 [hep-ph]].
- [75] A. Gando *et al.* [KamLAND-Zen], *Phys. Rev. Lett.* **117** (2016) no.8, 082503 [arXiv:1605.02889 [hep-ex]].
- [76] I. Esteban, M. C. Gonzalez-Garcia, A. Hernandez-Cabezudo, M. Maltoni and T. Schwetz, *JHEP* **01** (2019), 106 [arXiv:1811.05487 [hep-ph]].
- [77] F. R. Klinkhamer and N. S. Manton, *Phys. Rev. D* **30** (1984), 2212
- [78] V. A. Kuzmin, V. A. Rubakov and M. E. Shaposhnikov, *Phys. Lett. B* **155** (1985), 36